

Fullerene-based ruthenium catalysts: a novel approach for anchoring metal to carbonaceous supports. II. Hydrogenation activity

Th. Braun, M. Wohlers, T. Belz and R. Schlögl

Fritz-Haber-Institut der Max-Planck-Gesellschaft, Faradayweg 4-16, 14195 Berlin, Germany

Received 13 August 1996; accepted 22 October 1996

The influence of fullerenes and related support materials on the catalytic properties of ruthenium was investigated. The catalytic behaviour of catalysts based on C₆₀, raw fullerene black, extracted fullerene black, cathode deposit, and graphite was examined using low-temperature CO hydrogenation and liquid-phase hydrogenation of 2-cyclohexenone at atmospheric pressure. The relevance of non-six-membered carbon rings (NSMCR) in support materials on the stability and catalytic performance of the Ru particles will be illustrated.

Keywords: carbon support, fullerenes, fullerene black, cathode deposit, ruthenium, hydrogenation, CO, 2-cyclohexenone

1. Introduction

The quite unique catalytic properties of ruthenium, especially concerning hydrogenation reactions, are well known. It is the most active transition metal in the CO hydrogenation [1] and the hydrogenation of aliphatic carbonyl compounds [2]. Furthermore, the application of ruthenium in ammonia synthesis [3] and in various selective hydrogenation reactions [2] is of significant interest, especially the hydrogenation of α,β -unsaturated carbonyls [2,4]. The catalytic properties of the commonly applied supported ruthenium catalysts are affected by many factors such as the type of the metal precursor, the preparation procedure, and the support material [5–10]. Carbonaceous materials bind active metals usually via heteroatoms. Graphitic carbons exhibiting a low abundance of the latter are normally considered as inert support materials. Due to the proposed weak or lacking interaction with the support, the metal dispersion depends then on the geometrical parameters.

The first part of this contribution revealed that fullerenes and related polymeric substances (e.g. fullerene black and cathode deposit) are suitable support materials for ruthenium [11]. The unique structural feature of these substances is the presence of carbon rings not containing six carbon atoms. By altering the reactivity of their adjacent carbon–carbon double bonds, these NSMCR enable the formation of η^2 -type metal–carbon bonds, suitable for anchoring ruthenium directly to the support. The relative abundance of NSMCR dominates the structure and the stability of the ruthenium species in the investigated catalysts. The high reactivity of C₆₀ with respect to ruthenium caused by the high NSMCR abundance led to the formation of a branched network built of C₆₀ units which are interlinked by chemically bonded

Ru_x(CO)_y clusters. Analogous ruthenium species were detected in raw fullerene black, which is known to contain up to 11% extractable molecular fullerenes. The ruthenium species in extracted fullerene black were found to be Ru_x(CO)_y clusters bonded to the support. On graphite and cathode deposit metal-like and oxide-like ruthenium species were most abundant. On cathode deposit the preferred bonding sites were pocket-like structures and NSMCR inside them. The unusual geometrical irregularities are a direct consequence of the presence of NSMCR precluding parallel stacking of graphene structural elements.

In this study the hydrogenation behaviour of Ru/C catalysts is examined in order to elucidate the specific influence of C₆₀ (Ru₃C₆₀), raw fullerene black (Ru-FB_{raw}), extracted fullerene black (Ru-FB_{ex}), cathode deposit (Ru-CD), and graphite (Ru-AFS) on the catalytic properties of ruthenium.

Low-temperature CO hydrogenation (473–573 K) allowed the analysis of structural changes of the catalysts induced by thermal treatment in reductive atmosphere, whereas the selective hydrogenation of 2-cyclohexenone at 310 K enabled the investigation of the catalysts under mild conditions which are likely to preserve the initially present metal species.

2. Experimental

The catalysts were prepared by a combined impregnation–activation procedure (see part I [11]) based on the thermally induced reaction of Ru₃(CO)₁₂ with the respective support in boiling toluene.

CO hydrogenation was done at atmospheric pressure in a fixed-bed flow reactor. The catalysts were mixed with inert glass spheres (diameter 1 mm) to retain a cat-

alyst bed of 2 cm length which was fixed in the quartz reactor (inner diameter 8 mm) by quartz wool plugs. The CO consumption was kept well below 10% by choosing an appropriate catalyst amount. The absence of diffusion limitations was confirmed by variation of the feed gas flow rate.

The CO hydrogenation was performed at each reaction temperature until the product selectivity was constant and changes of the activity were well below 0.2% within an hour (steady state). After subsequent determination of the activation energy and the catalytic behaviour at 473 K the temperature was raised.

Oxygen and water traces in the high-purity feed gases (Linde) were removed by Oxisorb units (Messer Griesheim). Electronic mass-flow controllers were used to regulate the flow rates of CO (5 ml/min) and H₂ (15 ml/min). Analysis of the product gases was continuously performed with an on-line GC-system (Carlo Erba HRGC 3500) equipped with two columns (Haysep D (HWD), SPB 1 (FID)) for the determination of permanent gases and hydrocarbons containing up to eight carbon atoms. Additional GC-MS (Hewlett Packard G1800A GCD system; HP-5 capillary column) investigations enabled the identification of trace components of the product gases.

The liquid-phase hydrogenation of 2-cyclohexenone (310 K; hydrogen pressure 1 atm) was performed in a 100 ml flask connected to an apparatus (Adolf Kühner AG) providing a hydrogen reservoir at constant pressure. The weight of catalysts was chosen to retain 15 μ mol ruthenium. After 50 ml tetrahydrofuran (THF Merck p.a.) had been added to the catalyst the residual air in the flask was removed by five-fold evaporation and subsequent purging with argon. The stirred (500 rpm) suspension was saturated with hydrogen (Linde 99.999% purity) at 310 K for 12 h after the argon atmosphere was removed. Following the injection of 300 μ mol 2-cyclohexenone (Fluka > 95%) through a septum the progress of the reaction was monitored by the hydrogen consumption and GC-MS analysis (Hewlett Packard G1800A GCD system; HP-5 capillary column).

3. Results

3.1. CO hydrogenation

The catalytic activity of the carbon/ruthenium catalysts was tested in the CO hydrogenation between 473 and 573 K. The CO consumption was determined by summation of carbon-containing reaction products. Analysis of the product distribution by GC-MS revealed oxygenated hydrocarbons (methanol, ethanol) to be minor trace components. The oxygen generated by the dissociation of CO reacted predominantly to water. The formation of carbon dioxide in amounts well below

4 mol% of the carbon-containing products commenced at temperatures above 498 K on all catalysts.

The CO conversion rates are based on the total ruthenium content of the respective catalysts, because the exact determination of the number and the nature of the present active sites is difficult due to the structural changes of the catalysts during the CO hydrogenation. These structural changes are responsible for the observed complexity of the temperature dependencies of the catalytic behaviour. The proceeding structural changes of the active species did also affect the catalytic behaviour at a constant reaction temperature, as can be seen in fig. 1, revealing the changes with time and temperature in the CO conversion rates of the reference compound Ru₃C₆₀.

The activity data are summarised in figs. 2 and 3. The product selectivity to methane as represented by the ratio of methane formation to total hydrocarbon formation is shown in fig. 4. The catalysts can be separated according to their distinctly different reaction behaviour into two groups, Ru-CD and Ru-AFS on the one hand and Ru₃C₆₀, Ru-FBnex, and RU-FBex on the other hand.

Ru-AFS and Ru-CD exhibited a nearly exponential increase of the CO conversion at reaction temperatures up to 548 K (fig. 2). Raising the temperature to 573 K caused a pronounced decline of the catalytic activity of Ru-AFS whereas an increased CO conversion was observed for Ru-CD (fig. 2). The catalytic activity at 473 K (fig. 3) determined after previously applied high-temperature reaction (henceforth referred to as AHTR) revealed Ru-CD and Ru-AFS being the only catalysts that pass through an activation process during the CO hydrogenation. In the temperature range between 498 and 548 K the CO conversions at 473 K AHTR of Ru-CD and Ru-AFS increased to a maximum at 548 K which was nearly twice the initial value (fig. 3). This behaviour was ascribed to the formation of ruthenium metal particles by reductive processes leading to an increase of the active surface area thus enhancing the CO conversion rates. Agglomeration phenomena which pro-

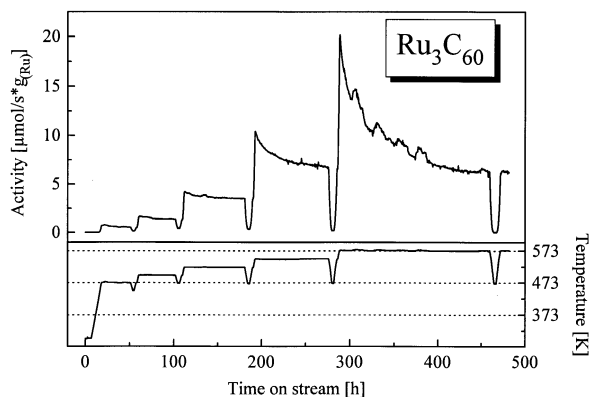


Fig. 1. Catalytic activity of Ru₃C₆₀ in the CO hydrogenation.

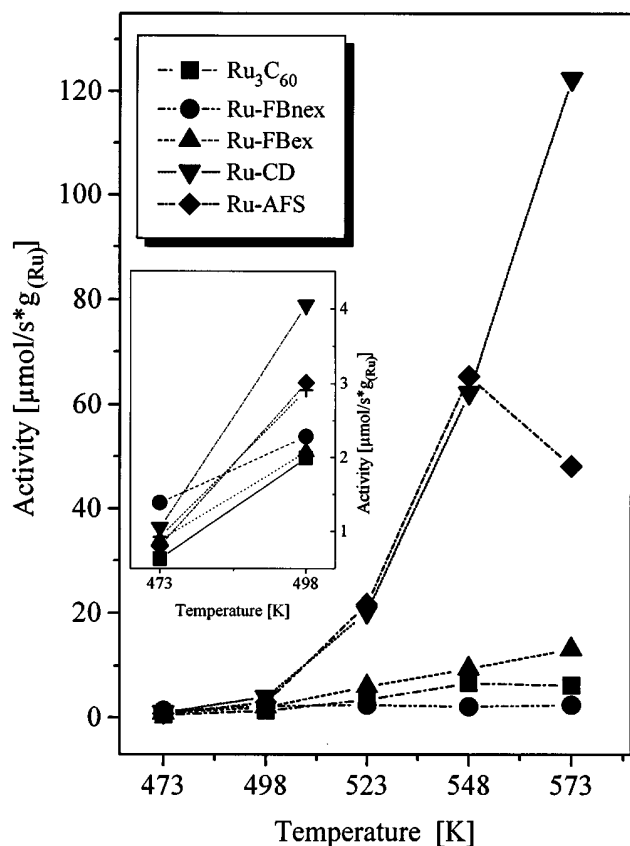


Fig. 2. Temperature dependencies of the steady-state CO conversion rates.

ceeded at 573 K extensively on Ru-AFS and less pronounced on Ru-CD induced a decrease of the catalytic activity at 473 K AHTR (fig. 3).

At reaction temperatures above 473 K Ru-CD and Ru-AFS are the most active catalysts investigated in this study. Their CO conversions at 548 K ($\sim 65 \mu\text{mol}/(\text{s g}(\text{Ru}))$) compare well to the values reported in the lit-

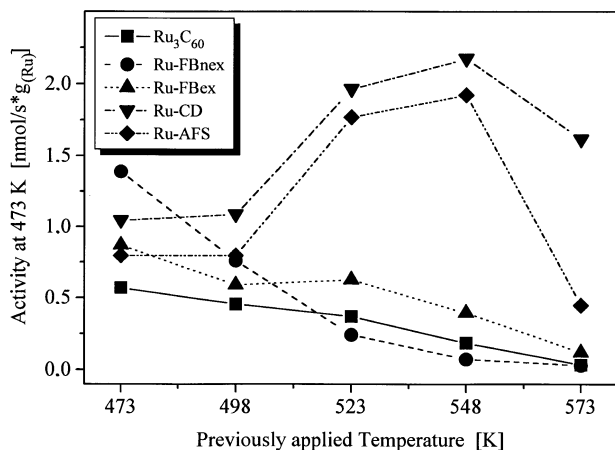


Fig. 3. Catalytic activities at 473 K versus previously applied reaction temperature.

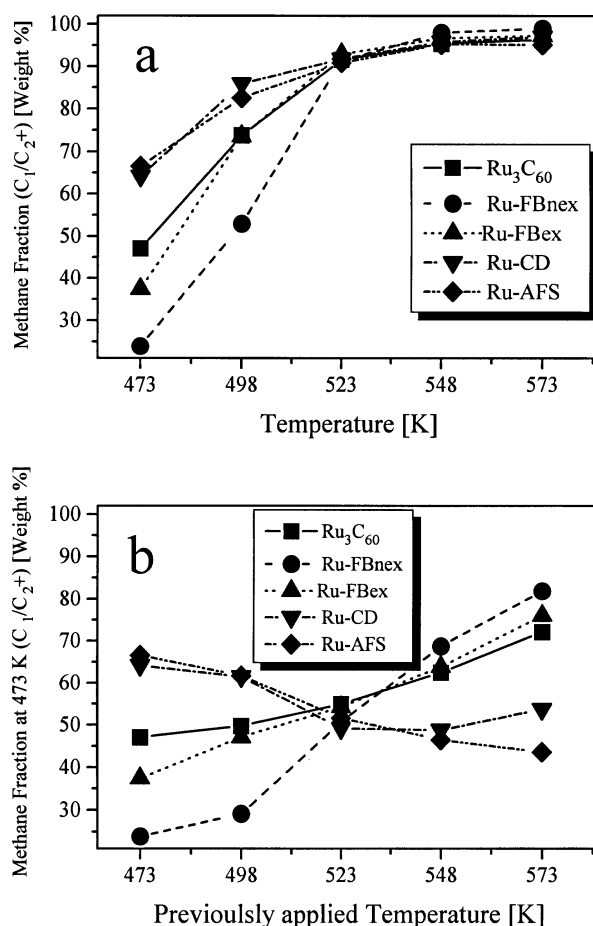


Fig. 4. Methane selectivity. (a) At a given reaction temperature, (b) at 473 K versus previously applied reaction temperature.

erature ($21\text{--}40 \mu\text{mol}/(\text{s g}(\text{Ru}))$) for catalysts consisting of highly dispersed ruthenium metal particles supported on carbon [12–14]. The slightly higher activities of Ru-CD and Ru-AFS were attributed to different sizes of the ruthenium particles in these catalysts. The activation energies for the CO conversion on Ru-CD (94 kJ/mol) and Ru-AFS (97 kJ/mol) determined after synthesis at 548 K also correspond to the values reported in the literature for metallic ruthenium supported on carbon (90–102 kJ/mol) [12,13]. These results pointed to the presence of metallic ruthenium in Ru-CD and Ru-AFS as active species.

In the temperature range investigated the selectivity to methane of Ru-CD and Ru-AFS (fig. 4a) was found to be lower compared to conventional carbon-supported ruthenium catalysts which are known to produce rarely higher hydrocarbons [12–15]. The decreasing methane selectivity at 473 K AHTR (fig. 4b) of Ru-CD and Ru-AFS was interpreted as an effect of the observed increasing particle size of the ruthenium metal [15].

For Ru₃C₆₀, Ru-FBnex, and Ru-FBex deactivation (fig. 3) was observed. The highest catalytic activity at 473 K of all investigated catalysts was determined for Ru-FBnex (fig. 2). The CO conversion rate approached

a nearly constant level at temperatures above 498 K (fig. 2). The activity at 473 AHTR (fig. 3) decreased rapidly due to irreversible structural changes of the active species caused by the formation of metallic ruthenium, as can be seen by TEM and EXAFS data of the used catalyst discussed in the first part of this contribution [11]. In the temperature range above 498 K Ru-FBex was found to be more active at a given reaction temperature and at 473 K AHTR than Ru₃C₆₀ which exhibited higher activities than Ru-FBnex.

The order of increasing activities corresponded to the determined order of decreasing crystallinity of the metallic ruthenium formed during CO hydrogenation. The conclusion that metallic ruthenium is the most abundant active species in the high-temperature regime was confirmed by the activation energies of the CO conversion at 548 K (Ru₃C₆₀ 102 kJ/mol, Ru-FBnex 94 kJ/mol, Ru-FBex 102 kJ/mol) and the high methane selectivity (fig. 4a) which correspond to the reported values of carbon-supported metallic ruthenium [12–15].

Compared to these conventional carbon-supported catalysts, Ru₃C₆₀, Ru-FBnex, and Ru-FBex exhibited strikingly different catalytic behaviours at low temperatures. At 473 K their selectivity for methane was found to be markedly lower, especially on Ru-FBnex (fig. 4a) which exhibited a lower value than unsupported ruthenium [14]. The proceeding transformation of the initially present active species into metallic ruthenium caused the decrease of this quite unique selectivity with increasing reaction temperatures (fig. 4a) and at 473 K AHTR (fig. 4b). Different onset temperatures and extents of this transformation were observed on Ru₃C₆₀, Ru-FBnex, and Ru-FBex pointing to differences in the deactivation kinetics.

3.2. Hydrogenation of 2-cyclohexenone

The low-temperature hydrogenation of 2-cyclohexenone is a better test reaction for the catalytic properties of the Ru/C catalysts without altering their structural characteristics than the high-temperature CO hydrogenation. On the one hand, reductive degradation pro-

cesses of the catalysts are unlikely to occur at the applied conditions, and on the other hand, ruthenium oxides which may be formed from small ruthenium metal particles are reduced at low temperatures [16].

Previous studies on the selective hydrogenation of α,β -unsaturated ketones [17] using Pt/SiO₂ and Ru/SiO₂ catalysts revealed the preferred hydrogenation of the carbon–carbon double bond in 2-cyclohexenone yielding cyclohexanone. The consecutive reduction of the carbonyl group leads to cyclohexanol. Formation of the unsaturated alcohol (2-cyclohexenol) was not observed.

Similar results were obtained in this work, as shown in table 1. Pristine Ru/C catalysts and samples used in hydrogen-chemisorption experiments (annealed at 673 K in vacuo and exposed to hydrogen at 293 K) were investigated to examine the initial catalytic properties and their variations with the pre-treatment. As no traces of 2-cyclohexenol were detected, the rate constants for the 2-cyclohexenone hydrogenation were calculated based on the 2-cyclohexenone concentration up to conversions of 80% assuming a first-order rate law with respect of 2-cyclohexenone. The rate constants are based on the amount of ruthenium (15 μ mol) and are given in μ mol/min. Using the normalised hydrogen consumption τ (τ = consumed moles H₂/moles 2-cyclohexenone at $t = 0$) the selectivity for cyclohexanone, S_{on} (S_{on} = moles cyclohexanone/moles cyclohexanol) was determined at $\tau = 1$. The observed induction period for the formation of cyclohexanol and the high selectivity for cyclohexanone at $t = 1$ (table 1) pointed to a consecutive hydrogenation mechanism.

Whereas all catalysts exhibited a high selectivity for cyclohexanone, strikingly different rate constants were observed. The activity of the pristine catalysts increases in the order Ru₃C₆₀ < Ru-FBnex < Ru-FBex < Ru-CD < Ru-AFS. The pre-treated samples exhibited a similar order of increasing activity Ru₃C₆₀ < Ru-FBnex < Ru-AFS < Ru-FBex < Ru-CD. The relative reaction rates with treatment given in fig. 5 clearly reveal that annealing significantly increased the activity of Ru₃C₆₀, RuFBnex, and Ru-FBex, whereas the activity

Table 1
Reaction rates and selectivities of the 2-cyclohexenone hydrogenation (310 K; 300 μ mol 2-cyclohexenone; 15 μ mol Ru)

Sample	Support	Ru ^a (wt%)	Pristine catalysts		After pre-treatment	
			rate constant ^b	selectivity ^c	rate constant ^b	selectivity ^c
Ru ₃ C ₆₀	C ₆₀	20	0.57	29	8.1	33
Ru-FBnex	not extracted	3.5	1.58	51	14	24
	fullerene black					
Ru-FBex	extracted	4	13.9	82	39	37
	fullerene black					
Ru-CD	cathode deposit	2	133	37	50	50
Ru-AFS	AFS-graphite	2.8	156	50	36	70

^a Determined by X-ray fluorescence analysis.

^b μ mol/min.

^c Moles cyclohexanone/moles cyclohexanol at $\tau = 1$.

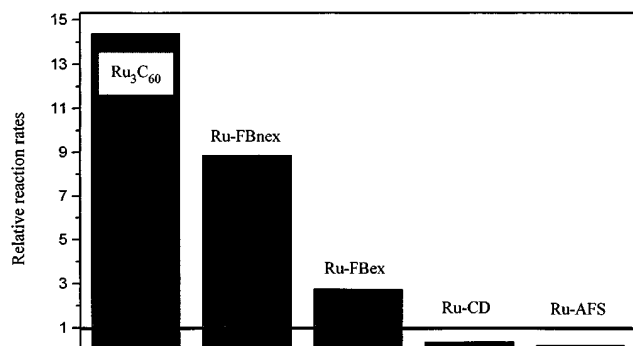


Fig. 5. Relative reaction rates of the 2-cyclohexenone hydrogenation (rate pre-treated catalyst / rate pristine catalyst).

of pre-treated Ru-CD and Ru-AFS decreased. The separation into two groups again corresponds to the observed behaviour in the CO hydrogenation and to the characterisation results (part I [11]).

Previous studies on the effect of the ruthenium dispersion on the hydrogenation of citral [8] and cinnamaldehyde [10] over Ru/C catalysts revealed a constant specific activity of ruthenium. Therefore, the observed differences in the reaction rates of the investigated catalysts can be caused either by the specific activity of the present ruthenium species, or by the number of catalytically active ruthenium atoms. In good accordance with EXAFS and TEM data of annealed samples (part I [11]) and the behaviour during CO hydrogenation, enlarged metal particle sizes in Ru-AFS and Ru-CD were assumed to reduce the activity after annealing. The relative reaction rates given in fig. 5 pointed to enhanced agglomeration of ruthenium on Ru-AFS compared to Ru-CD leading to stronger deactivation.

As the diameter of the ruthenium particles in pristine Ru-CD and Ru-AFS is similar to the most abundant $\text{Ru}_x(\text{CO})_y$ clusters (2–3 nm) in pristine Ru_3C_{60} , Ru-FBnec, and Ru-FBex, the low activity of the latter cannot be attributed to particle size effects. Presumably residual CO ligands and chemical bonding to the support material reduce the amount of potentially active sites. This hypothesis was supported by the observed higher activity of annealed samples, where CO desorption and commencing restructuring processes (part I [11]) increased the number of accessible ruthenium atoms. However, changes of the specific activity caused by annealing could not be ruled out to affect the enhanced reaction rates.

4. Discussion

The investigation of the fullerene-based ruthenium systems with respect to their hydrogenation activities revealed them to be catalytically active at low and moderate temperatures without any pre-treatment. Two groups of catalysts exhibiting corresponding catalytic

behaviours were established: ruthenium on C_{60} (Ru_3C_{60}), raw fullerene black (Ru-FBnec) and extracted fullerene black (Ru-FBex) on the one side, ruthenium on cathode deposit (Ru-CD) and natural graphite (Ru-AFS; reference) on the other. This categorising perfectly matches the structural characterisation results of the catalysts presented in part I of this contribution [11]. Consequently, the catalytic behaviour of the catalysts was deduced to the support material inducing the properties of the present ruthenium species.

Compared to conventional Ru/C catalysts Ru_3C_{60} , Ru-FBnec, and Ru-FBex exhibited a higher selectivity for hydrocarbons in the CO hydrogenation at 473 K. At higher reaction temperatures this exceptional selectivity and the activities decreased irreversibly due to the transformation of the initially active $\text{Ru}_x(\text{CO})_y$ clusters into metal. HRTEM and EXAFS analysis of used catalysts confirmed the formation of ruthenium metal particles, whereas deactivation by carbon deposition or formation of ruthenium compounds (oxides or carbides) was excluded. The order of decreasing activity at 573 K $\text{Ru-FBnec} < \text{Ru}_3\text{C}_{60} < \text{Ru-FBex}$ corresponds to the increasing size and crystallinity of the ruthenium particles. The high abundance of reactive non-six-membered carbon rings (NSMCR) in Ru_3C_{60} and Ru-FBnec was assumed to facilitate the reductive degradation of the support material (part I of this contribution [11]), thus enhancing the agglomeration and crystallisation of ruthenium leading to the observed changes of the catalytic properties.

In contrast to reductive treatment at elevated temperatures, annealing of Ru_3C_{60} , Ru-FBnec, and Ru-FBex in vacuo induced the loss of residual CO ligands without causing extensive crystallisation. The evolved ruthenium species exhibited strikingly higher activities in the hydrogenation of 2-cyclohexenone than the initially present $\text{Ru}_x(\text{CO})_y$ clusters. This finding led to the assumption that the structural modification of the ruthenium species and thus their catalytic properties by appropriate pre-treatment might multiply the possible applications for Ru_3C_{60} , Ru-FBnec, and Ru-FBex.

The catalytic properties of Ru-CD and Ru-AFS in the CO hydrogenation revealed ruthenium metal as the active species. Both catalysts were more active at 548 K than conventional Ru/C systems. Whereas Ru-CD retained a high activity at 573 K agglomeration of ruthenium led to a pronounced deactivation of Ru-AFS. The observed higher stability of the ruthenium particles on Ru-CD against sintering was confirmed by investigation of pristine and annealed samples in the hydrogenation of 2-cyclohexenone. The low relative reaction rate of Ru-AFS indicated a decrease of the metal surface area due to agglomeration. These findings confirm the structural characterisation results, revealing cathode deposit to be a valuable support material. The coexistence of corrugated surfaces and NSMCR enables the preparation of catalysts which

stabilise a high dispersion of the supported metal at elevated temperatures.

Furthermore, structural variation of the cathode deposit either by pre-treatment or by altering the graphite evaporation conditions offers numerous possibilities to influence the catalytic behaviour of the resulting Ru/C systems. For instance, a Ru/nanotube catalyst based on cathode deposit exhibited a very high selectivity for the desired α,β unsaturated alcohol in the hydrogenation of cinnamaldehyde [18]. It should be mentioned that the reported location of the ruthenium particles on the outer surface of the carbon nanotubes in our point of view is rather unexpected.

Selective oxidation of the end caps with nitric acid allows the deposition of metals inside the carbon nanotubes [19]. The described procedure generates a substantial amount of surface acid groups by oxidation of reactive sites presumably containing NSMCR. Thus the surface chemistry of the cathode deposit can be drastically altered.

Subsuming it can be concluded that materials with a high NSMCR abundance (e.g. fullerenes and fullerene black) are suitable support materials for low-temperature applications but are sensitive to reductive degradation at elevated temperatures. These materials induce the formation of catalytically active $\text{Ru}_x(\text{CO})_y$ clusters which can be modified by thermal treatment.

The low abundance of NSMCR in cathode deposit favours the formation of catalytically active ruthenium metal. The stability of cathode deposit against reductive degradation in combination with the mesostructure of the carbon material preserves the high dispersion of ruthenium at elevated temperatures.

Acknowledgement

This work was supported by the Bundesministerium für Bildung und Forschung through its fullerene programme.

References

- [1] M.A. Vannice, *J. Catal.* 37 (1975) 449.
- [2] P. Kluson and L. Cervený, *Appl. Catal. A* 128 (1995) 13.
- [3] S.R. Tennison, in: *Catalytic Ammonia Synthesis: Fundamentals and Practice*, ed. J.R. Jennings (Plenum Press, New York, 1991).
- [4] L. Mercandante, G. Neri, C. Milone, A. Donato and S. Galvagno, *J. Mol. Catal.* 105 (1996) 93.
- [5] Y. Issawa, *Catal. Today* 18 (1993) 21.
- [6] G.C. Bond, B. Coq, R. Dutartre, J. Garcia Ruiz, A.D. Hooper, M. Garcia Proietti, M.C. Sanchez Sierra and J.C. Slaa, *J. Catal.* 161 (1996) 480.
- [7] G. Neri, L. Mercandante, A. Donato, A.M. Visco and S. Galvagno, *Catal. Lett.* 29 (1994) 379.
- [8] S. Galvagno, C. Milone, A. Donato, G. Neri and R. Pietropaolo, *Catal. Lett.* 18 (1993) 349.
- [9] B. Coq, P.S. Kumbhar, C. Moreau, P. Moreau and M.G. Warawdekar, *J. Mol. Catal.* 85 (1993) 215.
- [10] S. Galvagno, G. Capannelli, G. Neri, A. Donato and R. Pietropaolo, *J. Mol. Catal.* 64 (1991) 237.
- [11] Th. Braun, M. Wohlers, T. Belz, G. Nowitzke, G. Wortmann, Y. Uchida, N. Pfänder and R. Schlögl, *Catal. Lett.* 43 (1997) 167.
- [12] J. Venter and M.A. Vannice, *Inorg. Chem.* 28 (1989) 1634.
- [13] M. Kaminsky, K. Joon, G. Geoffroy and M.A. Vannice, *J. Catal.* 91 (1985) 338.
- [14] M.A. Vannice and R.L. Garten, *J. Catal.* 63 (1980) 225.
- [15] A. Guerro Ruiz, J.D. Lopez Gonzalez and I. Rodriguez Ramos, *J. Chem. Soc. Chem. Commun.* (1984) 1681.
- [16] B. Coq, E. Crabb, M. Warawdekar, G.C. Bond, J.C. Slaa, S. Galvagno, L. Mercandante, J.G. Ruiz and M.C. Sanchez Sierra, *J. Mol. Catal.* 92 (1994) 107.
- [17] P. Geneste, M. Bonnet and C. Frouin, *J. Catal.* 64 (1980) 371.
- [18] J.M. Planeix et al., *J. Am. Chem. Soc.* 116 (1994) 7935.
- [19] R.M. Lago, S.C. Tsang, K.L. Lu, Y.K. Chen and M.L.H. Green, *J. Chem. Soc. Chem. Commun.* (1995) 1355.